Arch. Biol. Sci., Belgrade, 65 (4), 1363-1370, 2013 DOI:10.2298/ABS1304363M

EFFECT OF POTASSIUM OXALATE ON LIVER FUNCTION AND KIDNEY TISSUE OF DOGS (BEAGLES)

WALAA MOHAMADEN, HENG WANG, HUAWEI GUAN and JIANJI LI

Department of Animal Medicine, College of Veterinary Medicine, Yangzhou University, Yangzhou, Jiangsu, China

Abstract - Calcium oxalate crystalluria is a problem of growing concern in dogs. A few reports have discussed acute kidney injury by oxalates in dogs, describing ultrastructural findings in particular. We evaluate the possibility of deposition of calcium oxalate crystals in renal tissue and its probable consequences. Six dogs were intravenously injected with 0.5 M potassium oxalate (KOx) for seven consecutive days. By the end of the experiment, ultrasonography revealed a significant increase in the renal mass and renal parenchymal echogenicity. Serum creatinine and blood urea nitrogen levels were gradually increased. The histopathological features of the kidneys were assessed by both light and electron microscopy, which showed CaOx crystal deposition accompanied by morphological changes in the renal tissue of KOx injected dogs. Canine renal oxalosis provides a good model to study the biological and pathological changes induced upon damage of renal tissue by KOx injection.

Key words: CaOx, beagles, kidney, serum, SEM, TEM

RETRACTED

INTRODUCTION

The role of oxalate in renal crystal formation and its adverse effects are not completely clear. Some authors have stated that oxalates are poorly soluble in the presence of calcium, which causes them to precipitate as calcium oxalate crystals in the kidney tissue (Cruzan et al., 2004). Consequently, increased oxalate concentrations and crystal deposition in the tubules produces necrotic damage by inducing proximal tubular cell (PCT) death in rats (Thamilselvan and Khan; Guo and McMartin, 2005). Guo et al. (2007), using tissue culture, confirmed that oxalate in the form of calcium oxalate monohydrate (COM) is cytotoxic and increases the release of renal injury markers. Even when there is no crystal deposition, hyperoxaluria induced apoptotic changes in distal convoluted tubules (DCT) and collecting ducts (CD) in rabbit (Sarica et al., 2001). These dead renal epithelial cells may act as a nidus for the accumulation and aggregation of crystals in the tubules with the possibility of formation of mini-stones of CaOx (Khan, 2004). Oxalate crystal deposition tracks the inflammatory markers or mediators (Thamilselvan and Khan, 1998) and activates the expression of some interleukins and cytokines during the process of nephrolithiasis, inducing inflammatory conditions (Okada et al., 2010).

In the last couple of decades the incidence of CaOx urolithiasis has become a common problem in dogs worldwide (Houston and Moor 2009; Vrabelova et al., 2011). The most common causes are changes in the lifestyle of dogs, such as increased feeding with acidified commercial diets, changes in the dietary mineral content, especially calcium and magnesium, and changes in owner preferences as most people favor the small breeds of dogs, instead of larger breeds,

which are more prone to CaOx urolithiasis (Houston and Moor, 2009).

In order to investigate the clinicopathological effect and histopathological changes of CaOx urolithiasis in dogs, scientists have found different methods to induce CaOx crystals in dogs, mainly using oral administration of ethylene glycol (EG), which was found to be "ethically" unacceptable because of the severe signs of distress and pain it caused (Thrall et al., 1985; Smith et al., 1990). Furthermore, most studies into CaOx nephrolithiasis were conducted in either mice (Khan and Gelenton, 2010), rats (Khan et al., 2007) or tissue cultures (Ouyang et al., 2011), which makes the obtained results "impractical" for the field of veterinary medicine. In the same light, the studies that investigated all the biochemical, histological and ultrastructural changes accompanying CaOx nephrolithiasis in veterinary practice are rare in pets, although nephrolithiasis leads to significant renal injury and renal failure.

Our aims were to test the effect of an alternative oxalate precursor. potassium oxalate on crystal-deposition induction in dog kidneys. At the same time we wanted to evaluate the body response through an assessment of the liver and kidney functions and to report on the consequent ultrastructural renal changes that could help in unveiling the changes occurring in the course of nephrolithiasis.

MATERIALS AND METHODS

Experimental design

Ten healthy intact adult beagles with an age range 2.5-3 years were used in this study. Four dogs (one male and three females) were grouped as the control and the other six dogs (four males and two females) were considered the treatment group. All dogs were given 10 days for acclimatization and fed a dry, nutritionally complete dog food twice daily. Before starting the study, all dogs received a veterinary examination and had no previous history of long-term illness. Tap water was provided *ad libitum*. Each animal had a butterfly catheter fixed in the cephalic vein. Both groups were injected with the corresponding solution three times a day for seven consecutive days: physiological saline (0.9% sodium chloride NaCl) was administered to control dogs; 0.5 M potassium oxalate monohydrate ($K_2C_2O_4H_2O$ or KOx; 0.13 ml/kg) in sterile distilled water (previously filtered by passing through 0.22 µm) and physiological saline (1 ml/kg) were administered to the dogs of treatment group. The dogs were euthanized after surgical collection of the kidneys.

All procedures were approved by the animal Care and Use Committee of Faculty of Veterinary Medicine of Yangzhou University.

Ultrasonographic examination

A real time-gray scale ultrasound curved array (convex) transducer with a 3.5~5 MHz. was used for ultrasound examination. Renal measurements were performed in the sagittal view, and animals were positioned in lateral recumbence. Each animal was examined for any abnormal lesions in the renal system. and the maximum bipolar lengths (BPL) and the maximum widths (MW) in the hilar region of the right and left kidneys were measured at the beginning and end of the experiment.

Biochemical analysis

Blood samples were collected from the cephalic vein of all dogs on days D0, D1, D3 and D5 (D0 = prior to injection). Serum was preserved at -20°C until analysis. Blood urea nitrogen (BUN), creatinine, alanine aminotransferase (ALT), aspartate aminotransferase (AST), calcium (Ca) and magnesium (Mg) were analyzed by AU 4800 (Backman, USA).

Tissue morphological examination

Eight hours after injection of the last dose, both kidneys were collected surgically and then the dogs were euthanized.

RETRACTED

Light microscopy

Sections of kidney tissue (4 μm thick) were fixed in 10% neutral-buffered formalin, routinely processed, embedded in paraffin, and stained with H&E, PAS and Pizzolato's stains. After staining, images were investigated with an inverted phase-contrast microscope (Leica, Germany) equipped with the Quick Imaging system.

Electron microscopy (EM)

Scanning electron microscopy (SEM): kidney tissues were cut into smaller pieces (1 mm^3) and placed in a primary fixation of 2.5% glutaraldehyde dehydrated in a graded series of ethanol and dried. After mounting, a conductive layer was sputter coated on the samples and examined with an S-4 800 II FESEM (Hitachi High-Technologies Co., Japan). Transmission electron microscopy (TEM): after fixation in 2.5% glutaraldehyde the tissue was washed several times in a 0.1 M PBS buffer (pH, 7.4), post fixed in 2% osmium tetroxide in the same buffer, dehydrated in a graded ethanol series, exposed to several changes of 100% acetone, and embedded in epoxy resin. Ultrathin sections of the embedded tissue were examined unstained under the electron microscope (CM100 microscope, Philips Company, Holland).

Statistical analysis

SPSS 16.00 software was used for all analyses. Paired t-test was used to compare kidney parameters in the same animal before and after injection. One-way ANOVA (Shapiro-Wilk test) and sphericity (Mauchly's test) were used. Results are shown as presented as the mean ± SEM. Bonferroni's *post hoc* test was used to identify specific differences. The level of significance at which the null hypothesis was rejected was P = 0.05.

RESULTS

Ultrasonographic findings

Ultrasonographic images revealed that after treatment with 0.5 M KOx, there was mild hyperechogenicity in both cortical and medullary renal tissue. There was a significant increase in the BPL (7.138±0.089 cm) of the left kidney than before injection (6.0517±0.089 cm), and its (MW) was changed from 2.58±0.11 cm before treatment to 3.70±0.07 cm after treatment. Similarly, the BPL of the right kidney was significantly increased from 5.60±0.13 cm to 6.55±0.18 cm, as was the MW (from 2.85±0.11 cm to 3.65±0.29 cm. In contrast, no significant differences were found in the BPL or MW of the left or right kidney of the control and there was no change in the renal echogenicity.

Serum analysis

There was no change in serum creatinine and BUN observed in the control group (Table 1). However, there was a significant gradual increase in the serum creatinine and BUN in the treatment group during D0, D1, D3, and D5 of injection as shown in Table 2. There was no change in the AST, ALT, Ca or Mg levels either in control or in the treatment groups.

Histopathological findings

Crystals reacted positively with Pizzolato's stain and were localized in the lumen of the PCT, DCT and CD (Fig. 1). Tissues with crystals had the most severe lesions, tubular dilatation and hydropic degeneration. Tubular cell necrosis was observed in areas free from crystals. CaOx crystals arrayed in a fan shape inside the tubular lumen and crystals were resting on the epithelial surface causing detachment of the microvilli and brush border. The medulla had multiple foci of mini-stones surrounded by congestion, focal fibrosis and lymphocytic infiltration. Some glomeruli had CaOx crystal aggregates inside the urinary space. H&E and PAS staining showed that a few glomeruli were atrophied and contained eosinophilic or pink-colored material inside the Bowman's capsule and inside the tubular lumen, as shown in Fig. 2. On the other hand, evaluation of tissue specimens collected from the control group of dogs that received physiological saline exhibited normal renal tissue appearance.

RETRACTED

Table 1. Serum concentrations of magnesium, calcium and liver and renal function tests in control dogs on days 0, 1, 3 and 5.

	Day 0	Day 1	Day 3	Day 5
AST(U/L)	43.333±6.009	40.667±5.457	30.333±2.906	34.667±2.333
ALT (U/L)	58.000	56.333±2.963	54.667±6.173	56.667±6.888
BUN (mmol/L)	6.327±0.970	5.247±0.375	5.280±1.203	6.500±1.570
Creatinine (µmol/L)	72.933±10.080	76.000±9.067	76.967±15.507	65.767±10.834
Mg (mmol/L)	0.970±0.078	0.890±0.030	0.860±0.065	1.333±0.485
Ca (mmol/L)	2.373±0.043	2.377±0.050	2.250±0.[illegible]7	2.347±0.035

(AST) aspartate aminotransferase, (ALT) alanine aminotransferase, (BUN) blood urea nitrogen, (Mg) magnesium and (Ca) calcium. Tables were given mean ± SEM.

Table2. Serum concentrations of liver and renal function tests, magnesium and calcium in dogs injected with 0.5M KOx on days 0, 1, 3, and 5.

	Day 0	Day 1	Day 3	Day 5
AST(U/L)	44.5±2.21[a]	36.82±3.[illegible][a]	44.12±3.56[a]	41.56±4.66[a]
ALT (U/L)	69.72±19.98[a]	[illegible]12[a]	66.32±23.42[a]	54.52±17.45[a]
BUN (mmol/L)	8.04±1.32[a]	9[illegible]±1.54[a]	15.44±2.03[b]	19.96±4.30[b]
Creatinine (µmol/L)	100.48±15.29[a]	118.4[illegible]±15.61[a]	163.76± 20.59[b]	206.78± 37.57[b]
Mg (mmol/L)	0.85±[illegible]6[a]	0.69±0.19[a]	0.96±0.08[a]	0.99±0.08[a]
Ca (mmol/L)	2.37±0.15	1.81±0.58[a]	2.61±0.10[a]	2.67±0.07[a]

(AST) aspartate aminotransferase, (ALT) alanine aminotransferase, (BUN) blood urea nitrogen. The results are presented as the mean ± SEM[(a;b)]. Within a row values with different superscripts are significantly different (P <0.05).

RETRACTED

Scanning electron microscopy

The SEM of kidney tissue shows that crystals were bound to the injured epithelial cells of the renal tissue in the treated dogs. Some glomeruli were torn and CaOx crystals had blocked the tubular lumen by aggregation and became localized (Fig. 3). Mini-stone formation was found in the medulla. X-ray analysis of these crystals revealed a high calcium concentration, carbon and oxygen indicating calcium oxalate crystals deposition. In contrast, normal tubules were observed in the control group and the X-ray analysis that did not record any presence of CaOx crystals.

Transmission electron microscopy

Ultrastructural abnormalities in the treated group were expressed as follows: excessive vacuoles distributed in the cytoplasm of PCT and DCT. Some PCT cells had clubbing of the microvilli, basal infolding, and mitochondria were trapped between some of the infolding. Mitochondria appeared collapsed, cutoff in the mitochondrial membrane. Rupture and lysis of tubular cells evidenced the discontinuity of the apical membrane and released of their contents into the lumen. Necrotic cells contained shrunken abnormal nuclei. Crystal ghosts appeared inside the cells

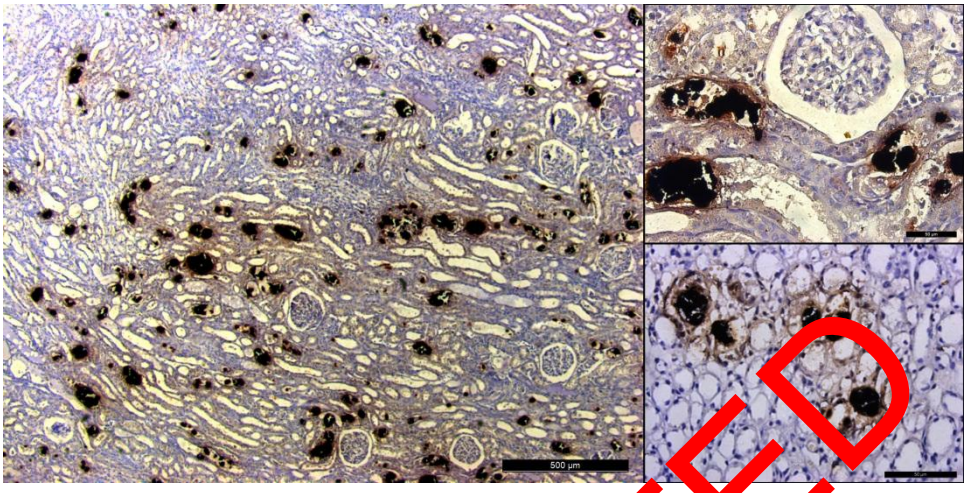

Fig. 1. Kidney sections staining Pizzolato-positive for crystals deposited in the lumen of the DCT and PCT. Bars = 500 µm & 50 µm.

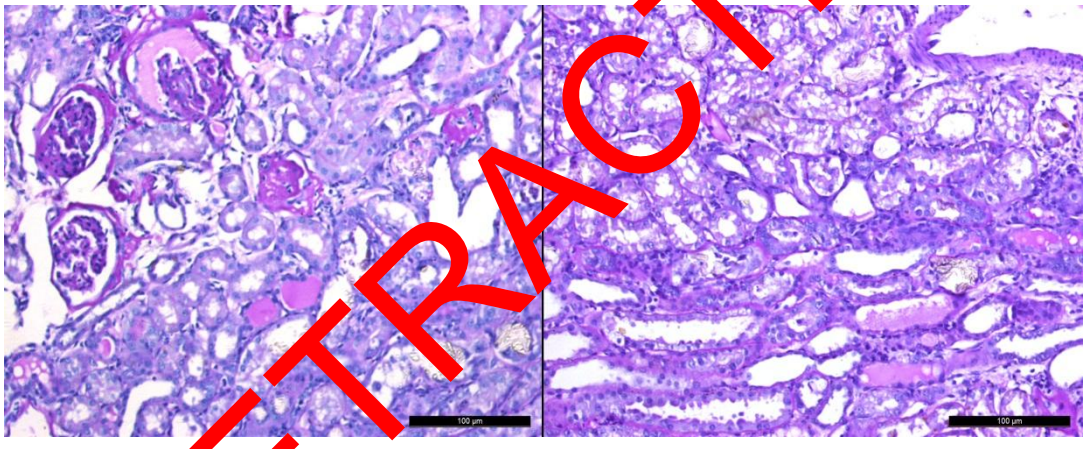

Fig. 2. Atrophied glomerulus with eosinophilic material in Bowman's capsule and in the tubular lumen. Bars = 100µm.

RETRACTED

and in the tubular lumen. Crystals were arranged in an alternative manner with the thick matrix (black layers) probably composed of protein and cell debris and crystal ghosts (white layers) as shown in Fig. 4. For the control group, TEM results revealed the normal appearance of the glomerular membrane, renal tubular cell and intact cellular contents.

DISCUSSION

Urine concentrations of oxalate and calcium play an important role in CaOx urolithiasis-formation in dogs. The process is associated with a complex and incompletely understood sequence of events. The changes that appeared in the treated group and were absent in the control group were due to the effect of KOx. Dog kidneys showed an increase in the echogenicity of the cortex and medulla. Two previous studies found the same results when dogs were administered with ethylene glycol (Adams et al., 1991), who attributed this to calcium oxalate crystal deposition within the kidney tissue. The renal mass of the experimental group was significantly increased after 7 days of KOx injection. This was manifested by the significant increase in the renal BPL and MW of both the right and left kidneys. Such an effect might be because of the early inflammatory condition accompanying CaOx crystal deposition in the kidney,

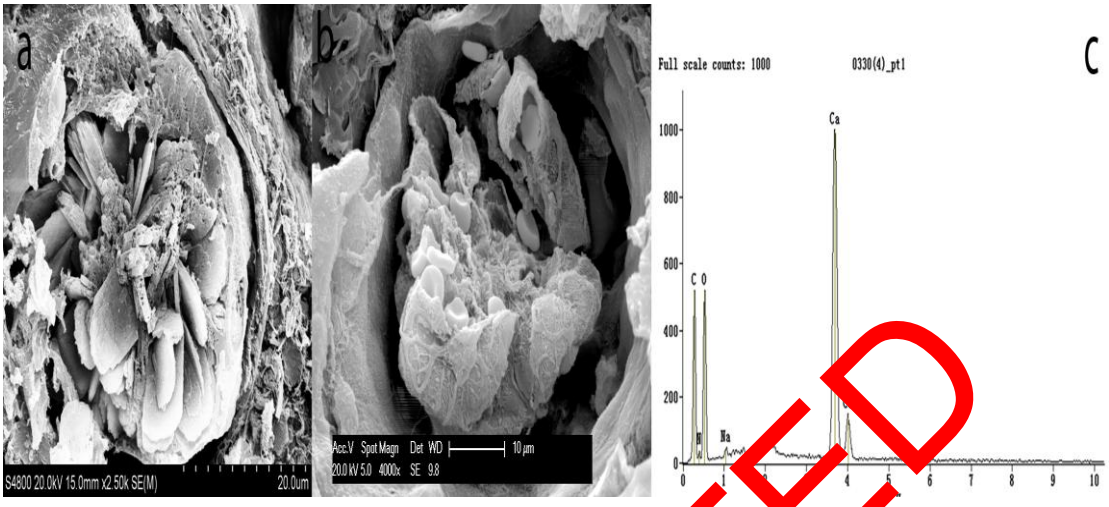

Fig. 3. SEM pictures of the kidney of the treated group. a) Aggregation of COM crystals arranged in a flower shape inside the lumen of DCT. Bar = 20 µm. b) Damaged glomerulus. Bar = 10 µm. c) X-ray analysis of the crystals with an elevated calcium content.

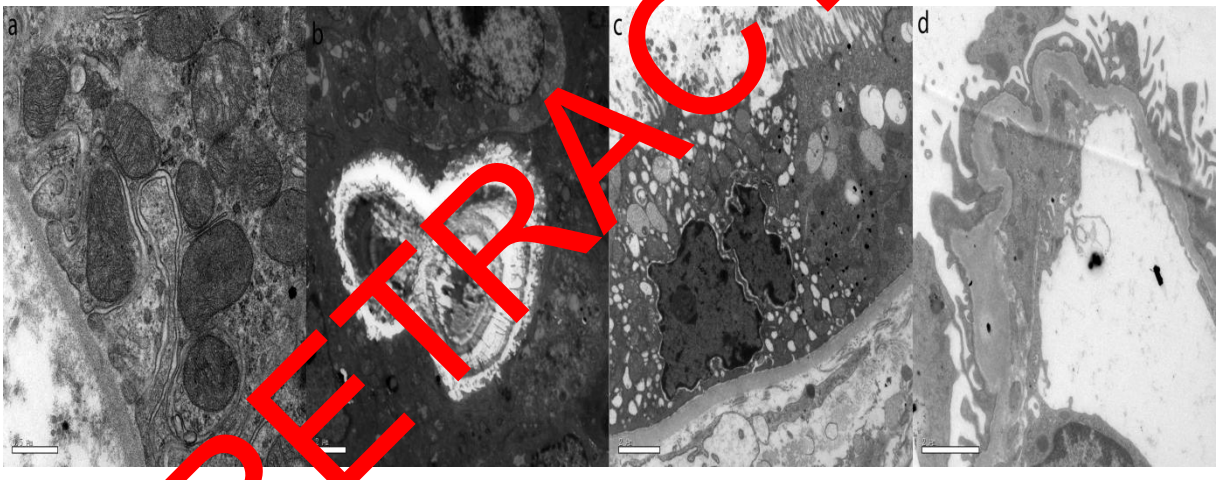

Fig. 4. Ultrastructure of the kidney of the treated group. a) Swollen and ruptured mitochondria bar = 0.5µm. b) Crystal ghost arranged in alternative manner with the black layer. Bar = 2 µm. c) Loss of the brush border and shrunk nucleus of the PCT. Bar = 2 µm. d) Irregular glomerular membrane. Bar = 2 µm.

RETRACTED

which was evidenced by the histopathological examination.

The significant gradual increase (Table 2) in both serum creatinine and BUN levels after KOx injection in this study indicates renal dysfunction (Emeigh Hart, 2005). Unlike other studies (Marengo et al., 2004), injection of rats with KOx did not induce any significant changes in either serum or urinary creatinine. The disturbances in normal kidney functions may occur due to the injurious effect of KOx on the kidney tissue with resultant renal crystal deposition, in addition to disruption of the normal filtration process that leads to retention of the toxic elements in the body.

In the present study, treatment of KOx injection led to crystals appearing in the lumen of PCT, DCT and CD (Fig.1), moving into inter- and intracellular locations and eventually into the interstitium. This

movement into the interstitium was associated with inflammatory conditions attracting many inflammatory cells including leukocytes, monocytes and macrophages. This interstitial infiltrate around the crystals might play an important role in renal tissue damage through the production of proteolytic enzymes, cytokines, and chemokines (Khan et al., 2002). At the intercellular level, the Pizzolato stain and TEM pictures of kidney tissue in this study revealed internalized crystals in cells, as observed by Schepers et al. (2005) after the continuous exposure of renal cells to oxalate crystals over 7 days of treatment.

The crystal retention and deposition that was clearly observed by SEM (Fig. 3) appeared to block the lumen surrounded by tissue debris and fibrous matrix. Crystal deposition and retention are not due to the lodgment of large-sized crystals inside the tubular lumen, but as a result of adhesion to injured cells that stimulates other crystals to collect (Asselman et al., 2003), which explains the relatively high expression of crystal-binding proteins such as osteopontin (OPN), hyaluronic acid (HA) and CD 44 (Hunter et al., 1998; Asselman et al., 2003). X-ray analysis confirmed that these crystals are only CaOx.

The TEM pictures of the treated group revealed renal epithelial-cell insult by the oxalate crystals, especially to those cells that appeared normal under light microscopy (Fig. 4). Similar observations have been made in other studies on ethylene glycol in dogs, rats and tissue cultures (MDCK) and oxalosis in cats (Smith et al., 1990; Schepers et al., 2003; Schepers et al. 2005; Khan, 2011; Niimi et al., 2012). Multiple basal infoldings inside the renal cell were suggested to coalesce together and form fewer large distensions that are likely related to the movement of extracellular fluid in the injured kidney (Smith et al., 1990). COM stone matrix were organized in arranged layers representing crystal ghosts which were observed inside and outside the renal cells as the crystals indeed became tightly embedded in the plasma membrane to ultimately end up inside these cells (Schepers et al., 2003). The crystal ghosts observed here were arranged radially in relation to the center, and contained an electron dense material resembling the structures described by Khan (2011) as CaOx crystal ghosts arranged as rosettes around a central nucleation site. In fact the crystal ghost is presumably formed by dissolution of COM crystals and the electron dense materials that are formed from cellular degradation products including degenerating nuclei, mitochondria, endoplasmic reticulum, and membrane fragments as well as vesicles occupying the inter-crystalline spaces (Khan, 2011). We considered that the electron dense matrix protected the rest of the renal epithelial tissue from direct contact with the crystals, which could be noticed from other cells and tubules even though they had no crystals in lumen. Mitochondrial collapse is very significant for calcium oxalate crystal deposition inside the renal tissue as mitochondria store considerable amounts of calcium ions that are discharged into the cytosol, causing further crystal buildup (Niimi et al., 2012).

Acknowledgments - This study was funded by the Priority Academic Program Development of Jiangsu Higher Education Institution (PAPD).

RETRACTED

REFERENCES

Adams, W.H., Toal, R.L. and *M.A. Breider* (1991). Ultrasonographic findings in dogs and cats with oxalate nephrosis attributed to ethylene glycol intoxication, 15 cases (1984-1988). *J. Am. Vet. Med. Ass.* **199**, 492-496.

Asselman, M., Verhulst, A., De Bore, M. E. and *C. F. Verkoelen* (2003). Calcium Oxalate Crystal Adherence to Hyaluronan-, Osteopontin-, and CD44-Expressing Injured/Regenerating Tubular Epithelial Cells in Rat Kidneys. *J. Am. Soc. Nephrol.* **14**, 3155–316.

Cruzan, G., Corley, R.A., Hard, G.C., Mertens, J.J. et al. (2004). Subchronic toxicity of ethylene glycol in Wistar and F344 rats related to metabolism and clearance of metabolites. *Toxicol. Sci.* **81**, 502-511.

Emeigh Hart, S.G. (2005) Assessment of renal injury in vivo. *J. Pharmacol. and Toxicol. Meth.* **52**, 30-45.

Guo, C. and *K.E. McMartin* (2005). The cytotoxicity of oxalate, metabolite of ethylene glycol, is due to calcium oxalate monohydrate formation. *Toxicol.* **208**, 347-355.

Guo, C., Cenac, T.A., Li, Y. and *K. E. McMartin* (2007). Calcium oxalate, and not other metabolites, is responsible for the renal toxicity of ethylene glycol. *Toxicol. Lett.* **173**, 8-16.

Houston, D. M. and *A. P. Moore* (2009). Canine and feline urolithiasis: Examination of over 50 000 urolith submissions to the Canadian Veterinary Urolith Centre from 1998 to 2008. *Can. Vet. J.* **50**, 1263-1268.

Khan, S.R., Johnson, J.M., Peck, A.B., Cornelius, J.G. and *P.A. Glenton* (2002). Expression of osteopontin in rat kidneys: Induction during ethylene glycol induced calcium oxalate nephrolithiasis. *J. Urol.* **168**, 1173-1181.

Khan, S. R. (2004). Crystal-induced inflammation of the kidneys: results from human studies, animal models, and tissue-culture studies. *Clin. Exp. Nephrol.* **8**, 75-88.

Khan, S. R., Glenton, P. A. and *K. J. Byer* (2007). Dietary oxalate and calcium oxalate nephrolithiasis. *J.Urol.* **178**, 2191-2196.

Khan, S.R. and *P. A. Glenton* 2010. Experimental induction of calcium oxalate nephrolithiasis in mice. *J.Urol.***184**, 1189-1196.

Khan, S.R. (2011). Renal cellular dysfunction/damage and the formation of kidney stones, In: P.N. Rao et al. (eds.) Urinary Tract Stone Disease, Springer-Verlag London Limited. 61- 86

Marengo, S. R., Daniel, H. C., Gregory, T. M., Martin, I. R. and *H. J. Gretta* (2004). Minipump induced hyperoxaluria and crystal deposition in rats: a model for calcium oxalate urolithiasis. *J. Urol.* **171**, 1304-1308.

Scheid, C. (2000). Oxalate toxicity in renal epithelial cells: characteristics of apoptosis and necrosis. *Toxicol. Appl. Pharmacol.* **162**, 132-141.

Niimi, K., Yasui, T. , Hirose, M., Hamamoto, S., Itoh, Y., Okada, A., Kubota, Y., Kojima, Y., Tozawa, K., Sasaki, S., Hayashi, Y. and *K. Kohri* (2012). Mitochondrial permeability transition pore opening induces the initial process of renal calcium crystallization. *Free Radic. Biol. Med.* **52**, 1207-1217.

Okada, A., Yasui, T., Fujii, Y., Niimi, K., Hamamoto, S., Hirose, M., Kojima, Y., Itoh, Y., Tozawa, K., Hayashi, Y. and *K. Kohri* (2010). Renal macrophage migration and crystal phagocytosis via inflammatory-related gene expression during kidney stone formation and elimination in mice: Detection by association analysis of stone-related gene expression and microstructural observation. *J. Bone Miner. Res.* **25**, 2701-2711.

Ouyang, J.M., Yao, X.Q., Tan, J. and *F. X. Wang* (2011). Renal epithelial cell injury and its promoting role in formation of calcium oxalate monohydrate. *J. Biol. Inorg. Chem.* **16**, 405-416.

Sarica, K.l., Yagei, F., Bakir, K.l., Erbaei, A., Erturhan, S. and *R. Ueak* (2001). Renal tubular injury induced by hyperoxaluria: evaluation of apoptotic changes. *Urol .Res.* **29**: 34-37

Schepers, M. S., Duim, R.A. , Asselman, M. , Romijn, J.C., Schröder, F.H. and *C. J. Verkoelen* (2003). Internalization of calcium oxalate crystals by renal tubular cells: A nephron segment-specific process. *Kidney Int.* **64**, 493-500.

Schepers, M. S., VanBallegooijen, E. S., Bangma, C.H. and *C.F. Verkoelen* (2005). Crystals cause acute necrotic cell death in renal proximal tubule cells, but not in collecting tubule cells. *Kidney Int.* **68**, 1543-1553.

Smith, B .J., Anderson, B. G., Smith, S. A. and *D. J. Chew* (1990). Early effect of ethylene glycol of ultrastructure of renal cortex of dogs. *Am. J. Vet. Res.* **51**, 89-96.

Thamilselvan, S. and *S.R. Khan* (1998). Oxalate and calcium oxalate crystals are injurious to renal epithelial cells: results of in vivo and in vitro studies. *J. Nephrol.* **11**, 66-69.

Thrall, M. A., Dial, S. M. and *D.R. Winder* (1985). Identification of calcium oxalate monohydrate crystals by X-ray diffraction in urine of ethylene. *Vet. Path.* **22**, 625-630.

Vrabelova, D., Silvestrini, P., Ciudad, J., Gimenez, J.C., Ballesteros, M., Puig, P. and *R. Ruiz de Gopegui* (2011). Analysis of 2735 canine uroliths in Spain and Portugal. A retrospective study: 2004-2006. *Res. Vet.Sci.* **91**, 208-211.

Yamate, T., Umekawa, T., Iguchi, M., Kohri, K. and *T. Kurita* 1998. Osteopontin antisense oligonucleotide inhibits adhesion of calcium oxalate crystals in Madin-Darby canine kidney cell. *J. Urol.***160**, 1506-12.

RETRACTED